

Photoelectron Diffraction in Magnetic Linear Dichroism

F. U. Hillebrecht,¹ H. B. Rose,¹ T. Kinoshita,^{1,*} Y. U. Idzerda,² G. van der Laan,³ R. Denecke,⁴ and L. Ley⁴

¹*Institut für Angewandte Physik, Heinrich-Heine-Universität Düsseldorf, 40225 Düsseldorf, Germany*

²*Naval Research Laboratory, Washington, D.C. 20375*

³*Daresbury Laboratory, Warrington WA4 4AD, United Kingdom*

⁴*Institut für Technische Physik II, Friedrich Alexander-Universität Erlangen, 91058 Erlangen, Germany*

(Received 28 March 1995)

The angular dependence of the magnetic linear dichroism in Fe and Co 3*p* photoemission is investigated. The dichroism has the same symmetry behavior as in the free atom, and vanishes when integrated over all angles. However, the angular dependence shows pronounced deviations from the $\sin^2\theta$ dependence of the free atom. The qualitative features can be understood in terms of a photoelectron diffraction picture, taking into account the details of the final state wave functions with respect to angular momentum and magnetic quantum numbers.

PACS numbers: 75.50.-y, 75.25.+z, 78.20.Ls, 79.60.-i

Core level photoemission spectroscopy can be turned into a surface sensitive probe for magnetic properties basically in two ways. The first is to employ spin analysis [1]. But, due to the large loss of signal in electron spin polarimetry, this route is a difficult one, and can only be applied to a fairly limited set of problems. The advent of magnetic dichroism in photoemission spectroscopy [2] has opened a second route. The discovery of a new type of magnetic linear dichroism [3] yielding information similar to circular dichroism has made magnetic sensitive photoemission spectroscopy feasible on almost any ordinary synchrotron radiation beam line. It is therefore timely to explore what new information can be obtained from the cross fertilization of magnetic dichroism with well-established and demonstrated photoemission techniques, such as photoelectron diffraction (PED) [4,5]. In this technique, one studies the variations of the angular emission pattern and its energy dependence of core level photoemission due to scattering by nearby atoms [4,5]. The attraction of PED lies in the possibility of obtaining information on structural properties in relation to, and simultaneously with, chemical information.

PED can be studied via the angle dependence, as well as via the photon energy dependence of a core level spectrum. In connection with magnetic dichroism, the latter method is not easily applicable because, apart from the scattering, there is a variation of the relevant matrix elements with energy that affects the dichroism. Therefore, the effect of PED on magnetic dichroism is more easily studied by investigating the angle dependence of photoemission spectra at fixed photon energies. In principle, there are two different sources of angular dependences of the magnetic dichroism. The first is due to the intrinsic angular dependence of the photoemission process, which depends on the relative orientation of sample magnetization, light polarization, and electron collection. This angle dependence can be inferred from an atomic model, and is often referred to as the source function. The second one is the geometrical structure around the emit-

ter: For crystalline materials, the measured core level photoemission intensity is enhanced or suppressed for emission along certain crystallographic directions due to photoelectron diffraction. Spin-dependent scattering has been observed in PED studies on antiferromagnetic Mn compounds via the emission angle dependence of the branching ratio between high and low spin Mn 3*s* final states [6]. The dependence of circular dichroism in Fe 2*p* photoemission on photon energy was also interpreted on the basis of spin-dependent scattering [7]. The importance of the emission direction for circular magnetic dichroism was realized when Schneider *et al.* [8] observed this effect for light helicity perpendicular to the sample magnetization.

In this Letter, we report on the magnetic linear dichroism as a function of the emission angle of the photoelectron for normal light incidence. Magnetic linear dichroism in the angular distribution (MLDAD) of photoelectrons requires a noncoplanar geometry of light polarization, electron detection, and magnetization direction. It is equivalent to the circular dichroism: In both cases the measured signal is proportional to the orbit spectrum I^1 , i.e., to the *orbital magnetization* of the magnetic sublevels [9]. Symmetry requires the effect to disappear in the total—i.e., angle-integrated—cross section, so that it can only be observed in an angle-resolved experiment. In order to obtain a comprehensive overview on the influence of photoelectron diffraction on the magnetic dichroism, we used a toroidal spectrometer capable of measuring the complete angular distribution in the plane normal to its axis [10].

Experiments were performed at the dedicated synchrotron radiation source BESSY in Berlin, using linearly polarized soft x rays from a crossed undulator beam line (U2-FSGM [11]). Fe and Co films were grown epitaxially on Ag(100) and Cu(100) in thicknesses of 70 and 15 monolayers, respectively, following procedures described in the literature [12,13]. Fe grows in the bcc structure on Ag(100), with the in plane [01] directions rotated by 45° to that of the substrate, while the growth of Co on Cu(100)

is pseudomorphic [13]. The magnetization was reversed by applying 80 Oe fields pulses along [01] for Fe, and [11] for Co. In a different set of experiments, microscopy of the total yield excited by circularly polarized light showed such films to be single domain; hysteresis loops measured by total yield were square, showing full saturation with the fields applied, and remanence virtually equal to saturation [14]. Because of the relatively large thicknesses, the Curie temperatures of these films can be assumed to be close to their bulk values [12,13]. The azimuthal and polar angular resolutions were about 3°, the total energy resolution was 0.3 eV.

Figure 1 shows the angle-resolved magnetic linear dichroism of the Fe 3*p* photoemission at 170 eV photon energy for normal incidence light and -45° emission angle (see the inset of Fig. 1). The dichroism manifests itself as a change in the Fe 3*p* line shape when the magnetization is reversed [3]. The lower panel of Fig. 1 shows the difference spectrum, compared to the result calculated within the model described in Ref. [9], with a spin-orbit splitting parameter of $\zeta_{3p} = 0.95$ eV, and a core exchange field H_s of 1.3 eV. To account for the finite lifetime and resolution, the theoretical spectra were convoluted with Lorentzians of 0.25 for spin-up and

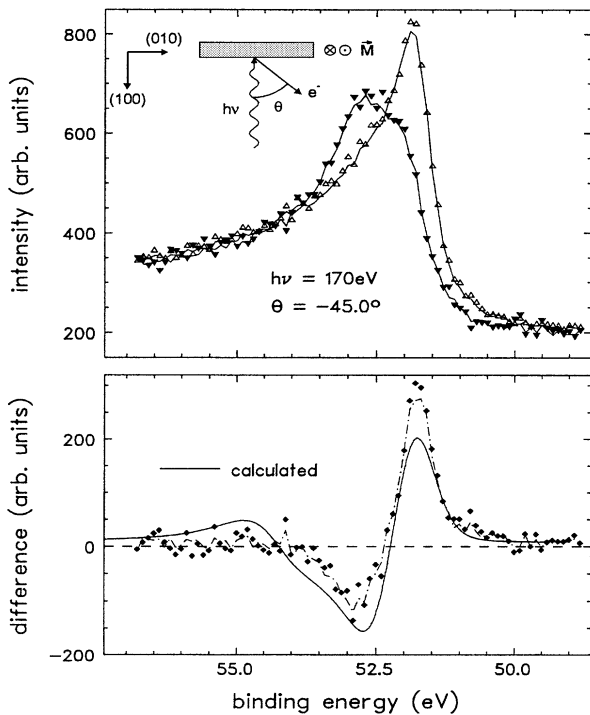


FIG. 1. Magnetic linear dichroism in angle-resolved Fe 3*p* photoemission ($h\nu = 170$ eV) for geometry as shown in sketch: light polarization is in the plane of the drawing, magnetization is in the surface normal to light polarization, electron emission is at -45°. Open and closed triangles correspond to magnetization up and down, respectively. Lower panel shows the difference spectrum compared to the calculated result.

0.9 eV for spin-down states, and a Gaussian of 0.3 eV. The spectral shape of the dichroism is in good agreement with the experimental result.

For a single free atom, the angular distribution of the dichroism for core *p*-shell emission is given by

$$J_{\text{MLDAD}} = (3/4\pi)I^1 \mathbf{P}(\boldsymbol{\epsilon} \times \mathbf{M})(\mathbf{P}\boldsymbol{\epsilon})R_s R_d \sin\delta, \quad (1)$$

where I^1 is the orbit spectrum, \mathbf{P} the polarization vector, \mathbf{M} the magnetization, $\boldsymbol{\epsilon}$ the unit vector in the direction of electron emission, and R_s and R_d the radial matrix elements for transitions into ϵ_s and ϵ_d continuum states with a phase difference δ . Consequently, MLDAD vanishes for $\boldsymbol{\epsilon}$ perpendicular or parallel to \mathbf{P} . For \mathbf{M} normal to \mathbf{P} , as in the present experiment, the angular dependence for a single atom is given by a $\sin 2\theta$ law.

Figure 2(a) shows the measured angular distribution of the photoemission intensity for both sample magnetizations at 51.8 eV binding energy, where the dichroism is maximum (see Fig. 1). Both emission patterns show four distinct features at $\pm 45^\circ$ and $\pm 20^\circ$ emission angles, whose shapes and intensities are affected by reversing the magnetization: The two emission patterns obtained by reversing the magnetization are mirror images of each other.

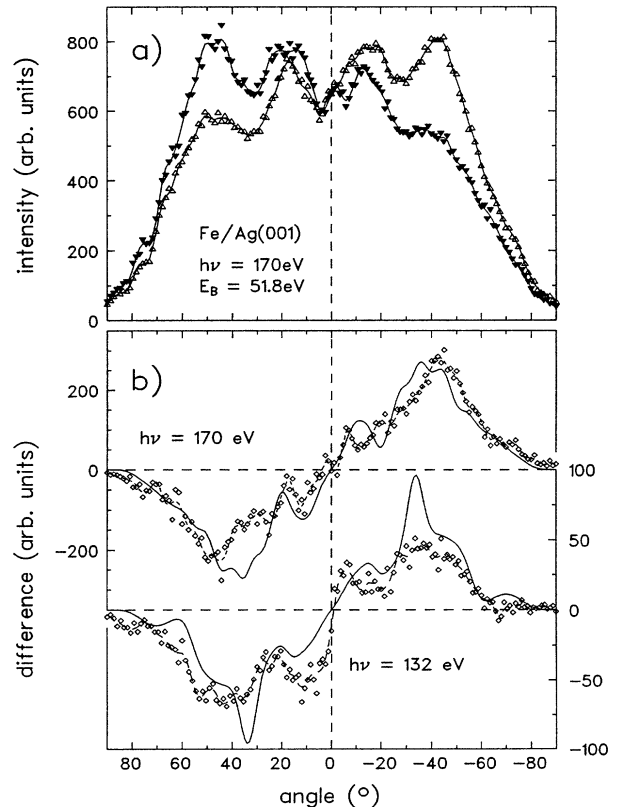


FIG. 2. (a) Fe 3*p* photoemission at 51.8 eV binding energy ($h\nu = 170$ eV) as a function of emission angle θ (see Fig. 1) for magnetization up (empty symbols) and down (full). Normal emission is at 0°. (b) MLDAD at 51.8 eV binding energy for 170 eV (left scale) and 132 eV (right scale) as a function of emission angle θ . Dashed lines are spline fits to guide the eye; full lines show results of single scattering calculation.

The rich structure in the angular distribution is in contrast to the slowly varying angular dependence for the free atom, and is caused by photoelectron diffraction.

The angular distribution of the magnetic linear dichroism, i.e., the difference between the two angular patterns in Fig. 2(a), is shown in Fig. 2(b). There is a small asymmetry with respect to reflection about the direction of normal emission, which we ascribe to the uncertainty in angle calibration and/or surface orientation. Apart from that, the linear dichroism has a similar angular dependence, but opposite sign for emission into the adjacent quadrants. This is also true for dichroism at other energies in the spectrum. Therefore, the total dichroism in the photoemission integrated over the emission plane vanishes. This shows for this plane that MLDAD occurs *only in angle-resolved photoemission*. For 132 eV photon energy, the diffraction pattern (not shown) has a pronounced peak in normal emission. The associated angular distribution of the dichroism (at the same binding energy) is also shown in Fig. 2(b).

Figure 3 shows an analogous set of results for Co/Cu(100) obtained with 148 eV photon energy, with the emission plane parallel to [11]. The dichroism is in general smaller than for Fe, as one may expect due to the smaller moment of Co. The largest dichroism occurs around $\pm 40^\circ$, and there is also a very large and strongly angle-dependent dichroism around normal emission. At $\pm 15^\circ$, the dichroism even changes sign over a small angle range.

The kinetic energies in these experiments are not high enough to ensure a general dominance of forward scattering in PED [3,4]. To understand the fine structure of the angular distribution of the dichroism in more detail, we performed calculations using a single scattering cluster model [15,16] with the inclusion of spherical wave corrections [17]. We used the Rehr-Albers formalism [16], which is a general electron-scattering formalism beginning with the separable free-electron Green's function propagator. This formalism, originally encoded by Friedman and Fadley [18], has been modified for arbitrary photon polarization and magnetization direction. For the present calculations, we used the unrelaxed bulk bcc Fe crystal structure and incorporated a single, spin-independent inelastic mean free path of 4 Å for these low energy photoelectrons (5 Å for Co), as well as the experimental energy and angular resolutions. Realistic variations of the inelastic mean free path, or inclusion of a slight spin dependence of the inelastic mean free paths, do not affect the overall shape of the calculated MLDAD.

The angular PED pattern is generated by combining all possible (l, m) final state waves, where l is the angular momentum and m the magnetic quantum number. In our geometry with the magnetization direction as the quantization direction, one has six possible final state waves for ionization out of a p state, $(0,0)$, $(2,0)$, $(2,\pm 1)$, and $(2,\pm 2)$. In principle, these waves have to be added coherently for comparison to the PED pattern. The $(2,\pm 1)$ partial waves have no emission intensity in this special configuration, so that different angular distributions arise

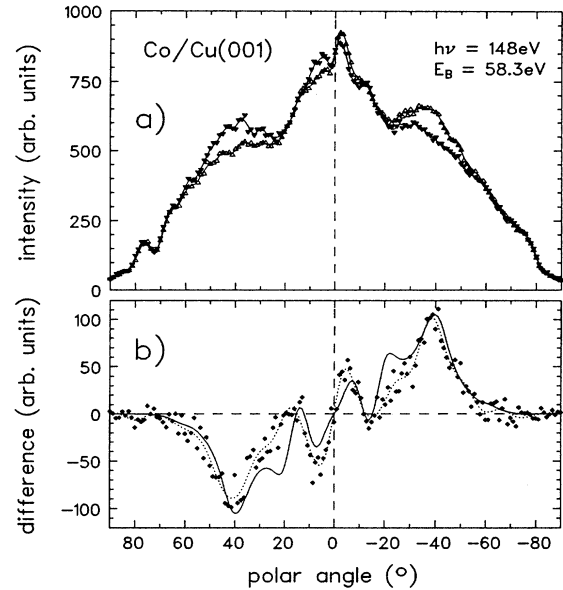


FIG. 3. (a) Angular distribution of Co 3p photoemission at 58.3 eV binding energy and $h\nu = 148$ eV for magnetization up (empty symbols) and down (full). Normal emission is at 0° . (b) MLDAD as a function of the emission angle for 58.3 eV binding energy. The dotted line is a spline fit to guide the eye; the full line gives the result of single scattering calculation.

from different contributions of $(2,\pm 2)$, the $(2,0)$, and $(0,0)$ partial waves. If no other information is at hand, the relative phases and amplitudes determining the shape of the pattern can be chosen appropriately by comparing to the experimental pattern. From our modeling we can say that for Co the $(2,0)$ final state contributes more at the energy of maximum dichroism than for Fe. In contrast to the diffraction pattern, the dichroism is determined exclusively by the $(2,\pm 2)$ final states, since the $(0,0)$ and $(2,0)$ partial waves are symmetric upon magnetization reversal.

The calculated angular dependences of the dichroism are compared to experimental results in Figs. 2(b) and 3(b). The calculation yields richly structured dichroism patterns, qualitatively similar to the measured ones. For the Co 3p data [Fig. 3(b)] there is very good agreement with the experimental data with respect to overall shape, or more specifically in terms of number, positions, and relative intensities of the structures of the angular distribution of the dichroism. The only exceptions are the shoulders at $\pm 20^\circ$, which are weaker in experiment than in the calculation.

For the higher photon energy Fe data shown in Fig. 2, the calculation yields a maximum dichroism at $\pm 36^\circ$, accompanied by structures of comparable strength at $\pm 25^\circ$ and $\pm 45^\circ$. The overall shape is similar to the experimental distribution that peaks at $\pm 45^\circ$, with shoulders on both sides. For the 132 eV Fe data one finds a broad distribution between $\pm 25^\circ$ and $\pm 50^\circ$, which is also seen in the measured distribution. However, the large structure at 33° is not observed in experiment. In view of the

good agreement obtained from the single scattering calculation for Co, it appears that the differences between experiment and calculation for Fe at low kinetic energy, where the sensitivity to structure and atomic composition is enhanced [19], is not due to neglect of multiple scattering, but to the structure of the Fe films.

To associate certain structures in the diffraction patterns with distinct scattering paths is difficult because of the strong nonforward scattering at low kinetic energies. In principle this might be done for photon energies as low as used here by performing calculations omitting certain atoms in the cluster. However, even though the individual angular distributions are quite different for Fe and Co, the difference distributions are expected to show some similarities in shape, but with shifted peak positions. This is because the structures of Fe and Co are related by a tetragonal distortion, and only the $(2, \pm 2)$ state contributes to the difference spectra (the others are symmetric). Such slight differences in peak positions are in principle directly relatable to the differences in the bond orientation angle of fcc vs bcc structures, if data taken with the same kinetic energy are available.

Beyond being sensitive to the local structure and chemical environment of each element of the material, the MLDAD angular patterns are, of course, sensitive to magnetic properties of the material. By focusing on the dichroism pattern, the sensitivity to the magnetic properties of the material is enhanced relative to influence of the structural properties, which dominates in normal PED. An extremely useful aspect is the influence of the m -sublevel occupation of the valence bands, and therefore to the orbital moment of the material, on the dichroism pattern [15]. Although we do not yet extract magnetic parameters, it is evident from the different Fe and Co angular distributions that the complementary structural and magnetic information is really contained in these data, making this a technique of great utility.

In summary, we have observed strong photoelectron diffraction effects in magnetic linear dichroism. The wealth of structure in the angular distribution of the magnetic dichroism can be understood by single scattering calculations. The primary source of the strong modulations is the dependence of the scattering not only on the angular momentum, but also on the magnetic quantum numbers of the continuum final state. The angular distribution pattern of the magnetic dichroism contains complementary information on the structure and the magnetic moments close to the surface, which will be extracted by more extended modeling. The combination of PED with magnetic dichroism promises to be a powerful tool to investigate the details of the magnetic structure at and near surfaces.

We are grateful to E. Kisker for support, and to G. Reichardt and A. Gaupp of BESSY for help in operating the beam line. Funding by the Bundesministerium für Forschung und Technologie (BMFT) under Grants No. 05

5PFDAB 3 and No. 05 5WEDA B3 as well as by the Deutsche Forschungsgemeinschaft (DFG/SFB 166/G7) is gratefully acknowledged. The participation of T. K. was supported by the Alexander von Humboldt Foundation.

*Humboldt fellow on leave from the Institute for Solid State Physics, University of Tokyo, Roppongi, Minato-ku, Tokyo 106, Japan. Present address: UVSOR, Institute for Molecular Science, Okazaki 444, Myodaiji, Japan.

- [1] C. Carbone and E. Kisker, *Solid State Commun.* **65**, 1107 (1988); F.U. Hillebrecht, Ch. Roth, R. Jungblut, E. Kisker, and A. Bringer, *Europhys. Lett.* **19**, 711 (1992).
- [2] L. Baumgarten, C.M. Schneider, H. Peterson, F. Schäfers, and J. Kirschner, *Phys. Rev. Lett.* **65**, 492 (1990).
- [3] Ch. Roth, F.U. Hillebrecht, H.B. Rose, and E. Kisker, *Phys. Rev. Lett.* **70**, 3479 (1993); *Solid State Commun.* **86**, 647 (1993).
- [4] C.S. Fadley, *Prog. Surf. Sci.* **16**, 275 (1984); in *Synchrotron Radiation Research: Advances in Surface Science*, edited by R.C. Bachrach (Plenum, New York, 1989).
- [5] W.F. Egelhoff, in *Ultrathin Magnetic Structures*, edited by J.A.C. Bland and B. Heinrich (Springer, Berlin, 1994).
- [6] B. Hermsmeier, J. Osterwalder, D.J. Friedman, B. Sinkovic, T. Tran, and C.S. Fadley, *Phys. Rev. B* **42**, 11 895 (1990).
- [7] G.D. Waddill, J.G. Tobin, X. Guo, and S.Y. Tong, *Phys. Rev. B* **50**, 6774 (1994).
- [8] C.M. Schneider, D. Venus, and J. Kirschner, *Phys. Rev. B* **45**, 5041 (1992); D. Venus, L. Baumgarten, C.M. Schneider, C. Boeglin, and J. Kirschner, *J. Phys. Condens. Matter* **5**, 1239 (1993).
- [9] G. van der Laan and B.T. Thole, *Solid State Commun.* **92**, 427 (1994); B.T. Thole and G. van der Laan, *Phys. Rev. B* **50**, 11 474 (1994).
- [10] R.C.G. Leckey and J.D. Riley, *Appl. Surf. Sci.* **22/23**, 196 (1985).
- [11] J. Bahrtdt, A. Gaupp, W. Gudat, M. Mast, K. Molter, W. B. Peatman, M. Scheer, Th. Schroeter, and Ch. Wang, *Rev. Sci. Instrum.* **63**, 339 (1992).
- [12] Z.Q. Qiu, J. Pearson, and S.D. Bader, *Phys. Rev. Lett.* **70**, 1006 (1993); *Phys. Rev. B* **49**, 8797 (1994).
- [13] C.M. Schneider, P. Bressler, P. Schuster, J. Kirschner, J.J. de Miguel, and R. Miranda, *Phys. Rev. Lett.* **64**, 1059 (1990).
- [14] D. Spanke, J. Dresselhaus, F.U. Hillebrecht, and E. Kisker (to be published).
- [15] Y.U. Idzerda and D.E. Ramaker, *Mater. Res. Soc. Symp. Proc.* **313**, 659 (1993).
- [16] J.J. Rehr and R.C. Albers, *Phys. Rev. B* **41**, 8139 (1990).
- [17] M. Sagurton, E.L. Bullock, R. Saiki, A. Kaduwela, C.R. Brundle, C.S. Fadley, and J.J. Rehr, *Phys. Rev. B* **33**, 2207 (1986).
- [18] D.J. Friedman and C.S. Fadley, *J. Electron. Spectrosc. Relat. Phenom.* **51**, 689 (1990).
- [19] T. Greber *et al.*, *Phys. Rev. Lett.* **69**, 1947 (1992); Y.U. Idzerda and D.E. Ramaker, *ibid.* **69**, 1943 (1992).